Review Article

Zeeshan*, Ilyas Khan, Amina, Nawa Alshammari, and Nawaf Hamadneh

Double-layer coating using MHD flow of third-grade fluid with Hall current and heat source/sink

https://doi.org/10.1515/phys-2021-0079
received August 30, 2021; accepted October 23, 2021

Abstract: Multiple coating assessments of fiber optics utilizing micropolar convection non-Newtonian third-order liquid in the existence of Hall effect are examined and executed throughout this academic article. The wet-on-wet (WOW) coating process is used in the research. The fourth Runge–Kutta–Fehlberg algorithm is used to computationally solve the governing equations which dictate the movement of fluid inside the container. In this research, the RK4-Fehlberg algorithm is applied to get numerical results for a list of nonlinear ordinary differential equations (ODEs) describing liquid motion. Pictorially, the contribution of regulating variables on velocity and temperature profiles is examined. It is observed that the velocity profile enhances as the viscoelastic parameter increases and the velocity profile increases for both the non-Newtonian and Hall current increasing parameters in the presence and absence of magnetic parameter M. It is observed that the velocity of the fluid decreases with the increasing values of the Hartmann number m, Brinkman number Br, and magnetic parameter M. Furthermore, the temperature profile increase for Br, K, M, and opposite effect is observed for β increases. The suggested approach is compared to homotopy analysis method (HAM) for verification purpose, and excellent agreement is obtained. In addition, as a restricted scenario, a connection is made with the existing literature.

Keywords: double-layer coating, numerical solutions, mathematical modeling, third-grade fluid, Hall current, magnetohydrodynamics (MHD) flow, heat source/sink

*** Corresponding author: Zeeshan,** Department of Mathematics and Statistics, Bacha Khan University Charsadda, KP, 24420, Pakistan, e-mail: zeeshansuit@gmail.com
Ilyas Khan: Department of Mathematics, College of Science, Al-Zulfi, Majmaah University, Majmaah, 11952, Saudi Arabia
Amina: Department of Mathematics and Statistics, Bacha Khan University Charsadda, KP, 24420, Pakistan
Nawa Alshammari, Nawaf Hamadneh: Department of Basic Sciences, College of Science and Theoretical Studies, Saudi Electronic University, Riyadh, 11673, Saudi Arabia

1 Introduction

The double layer coating technique insulates plastics using melted resins for structural rigidity and protection against harsh environments. Plastic polymers used during wire treatments include polyamide polysulfide, low/high density polyethylene (LDPE/HDPE), and plastic polyvinyl chloride (PVC). Coating for optical fiber is necessary because it protects the fiber from mechanical damage. The helix extruded methodology, which works at extreme pressure, heat, and fiber/wire drawing acceleration [1–4], is a suitable and simple method of fiber/wire coating. Pulse dies have a really close resemblance to a nucleus; the flow through them is similar to the flow through the concentric region formed by two concentric cylinders, with the inner cylinder rolling axially and the exterior cylinder being fixed. Different types of fluids were considered for the wire, depending on the shape of the die, fluid viscosity, wire range, and melted polymeric temperature. The Newtonian fluids have been treated with great care in order to explore the results of simulation in the metallic fabrication. Through science and technology, many fluids, such as air, liquid, and various lubricants, are being classified as non-Newtonian liquids. In many cases, Newtonian fluid behavior is not straightforward and will be more sophisticated, necessitating the use of a perturbation model. Non-Newtonian behavior can be found in a variety of liquids, including sticky oil, mustard crème, and plasma. Pharmaceutical and petrochemical engineering, and other quantum dynamics, have received much attention due to their wide and important applications in industry [5–9]. A non-Newtonian liquid in vein movement across laminate stenosis was addressed by Shah *et al.* [10]. Eyring–Powell fluid is indeed a non-Newtonian solvent first proposed by Eyring and Powell in 1944.

Owing to its relevance in the atomic and commercial sectors, the concept of two surfactant molecule streams involving heat exchange was already examined briefly. Stratified flows, transitioning or mixed flows, and diffused flows are the three types of flows. Shah *et al.* [11]

investigated the second-grade fluid for wire coating purpose. For cable and fiber optical covering, many varieties of solvents are utilized, depending mostly on sheet geometry, dynamic viscosity, wire or fiber optics heat, and melted polymeric temperature. The summary of the most vital work regarding wire and fiber optics treatment is as follows. Typical wire coating assessment was studied by Shah *et al.* [12] using linearly increasing temperature. Shah *et al.* [13] explored second-grade and third-grade liquids with an oscillation boundary condition in a wire coating die. Wire covering evaluation yielded accurate solutions for second-grade solvent. All these efforts were made in the context of a single-layer coating flow.

Numerous production and commercial activities, including the oil sector and polymer manufacture, rely on immiscible flowing fluid. Kim *et al.* [14] investigated a theoretically predicted dual coating with wet-on-wet (WOW) fiber optic production. Kim and Kwak [15] employed two-layer coating flow for optical fiber fabrication. The power-law flow method was established for this. With double-fiber optic coating, Zeeshan *et al.* [16] employed Phan-Thien Tanner fluid. Using a WOW coating procedure with a continuous hydrostatic pressure, Zeeshan *et al.* [17] examined twofold resin covering of optical fiber glass. Zeeshan *et al.* [18] utilized a multiple distribution of an Oldroyd 8-constant solvent for fiber optic treatment. Khan *et al.* [19] examined mass and heat diffusion in a dual fiber optic coating utilizing a WOW coating method.

Magnetosphere causes electricity in MHD, which has a significant impact upon the fluid material's mobility. The MHD has become a popular trend in the industry due to its widespread application in various industrial processes including the production of magnetic materials and glassware. Many studies [20–26] looked at MHD as a current-conducting material in the inclusion or exclusion of an electric field, as well as the repercussions of this.

The process of heat evacuation for non-Newtonian fluid has gained popularity throughout time as a result of its application in various sectors. Heat convection modeling involving nonlinear and nonstagnated flow movement was studied by Rehman and Nadeem [27]. The influence of natural radiation and micropolar flow velocity was investigated by many researchers [28–50]. The metal fiber coating approach incorporating MHD of a viscous Eyring–Powell solvent as coating ingredient is still to be explored, according to the above literature. So the novelty of this study is to investigate the Maxwell fluid and ambient temperature on the incompressible flow of a non-Newtonian (Erying–Powell) fluid wherein the optical fiber dragged at a higher velocity in the existence of Hall current is discussed in this investigation. Despite the fact that there may be various studies on the heat and mass transfer for non-Newtonian flows, a detailed review of the literature reveals that a viscoelastic fluid receives very little interest. Nobody has investigated the magnetohydrodynamic heat transfer characteristics of a viscoelastic fluid to characterize a double-fiber optic coating as far as we realize.

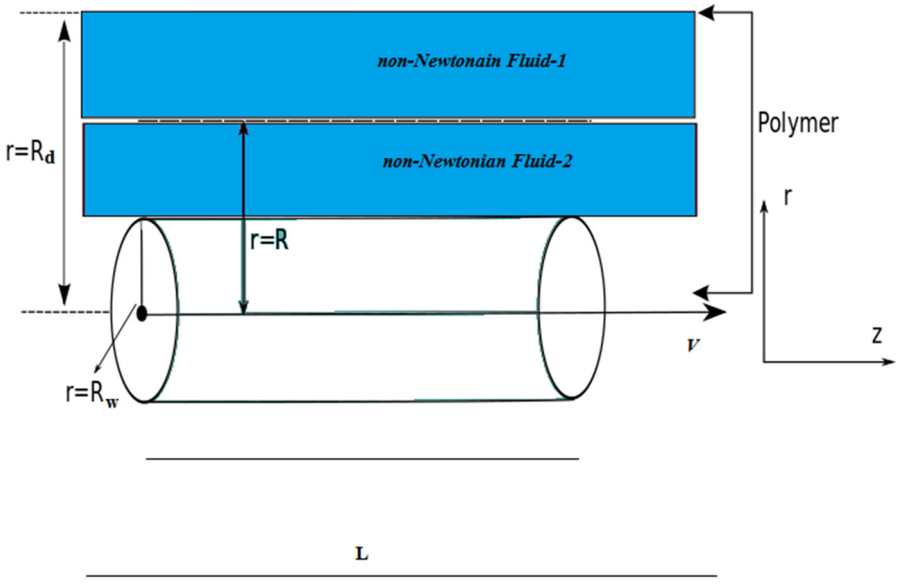

Figure 1: Geometry of the model problem.

The performance of heat transfer over non-Newtonian fluids has gained popularity as a result of its application in various sectors.

2 Mathematical analysis

For the surface coating, naked glass fiber is pulled into the centerline of a lacquer assembly's extruder at a speed V determined by fluid temperature θ_w and radius of fiber optics R_w in a pool of Maxwell fluid used as a molten polymer for encasing purposes such as PVC inside a stationary pressurized die of magnitude L, radius R_d, and temperature θ_d as depicted in Figure 1. It is assumed that the flow is laminar, incompressible, steady, and axisymmetric. The liquid operates under a constant axial differential pressure as well as a strong transversal magnetic field of strength B_0. A Reynolds number is kept as low as feasible in order to refute the resultant magnetic field.

Two common coating processes for optical fiber coating are WOW and WOD [14–19]. In WOD operation, the uncoated glass fiber penetrates the initial coating sprayer and the initial coating is quickly dried *via* UV rays from UV lamps. The virgin glass fiber penetrates both the primary and secondary spraying softeners at the same time mostly in WOW fabrication (Figure 2), and is subsequently cured by UV lights. Earlier, the WOD precipitation method [22] was employed mostly; however, the WOW fabrication technique has recently gained a lot of traction in the industrial sector.

The optical fiber and the die are symmetric in which the fiber is dragged at the center of the die along the flow direction. The coordinate system is choosen at the centre of the die. The motion is axisymmetric, constant, and smooth. Furthermore, the covering matrix's structure is more crucial because it has a significant impact on the final performance of the product. As a result, for the fiber optic surface coating, a pressurized coating type die is recommended. The velocity profile, extra stress tensor, and thermal fields are calculated using the above mentioned frame and constraints as follows:

The governing equations for the two fluids are as follows [14–19]:

Continuity equation

$$\nabla . \upsilon^{(\varphi)} = 0. \tag{1}$$

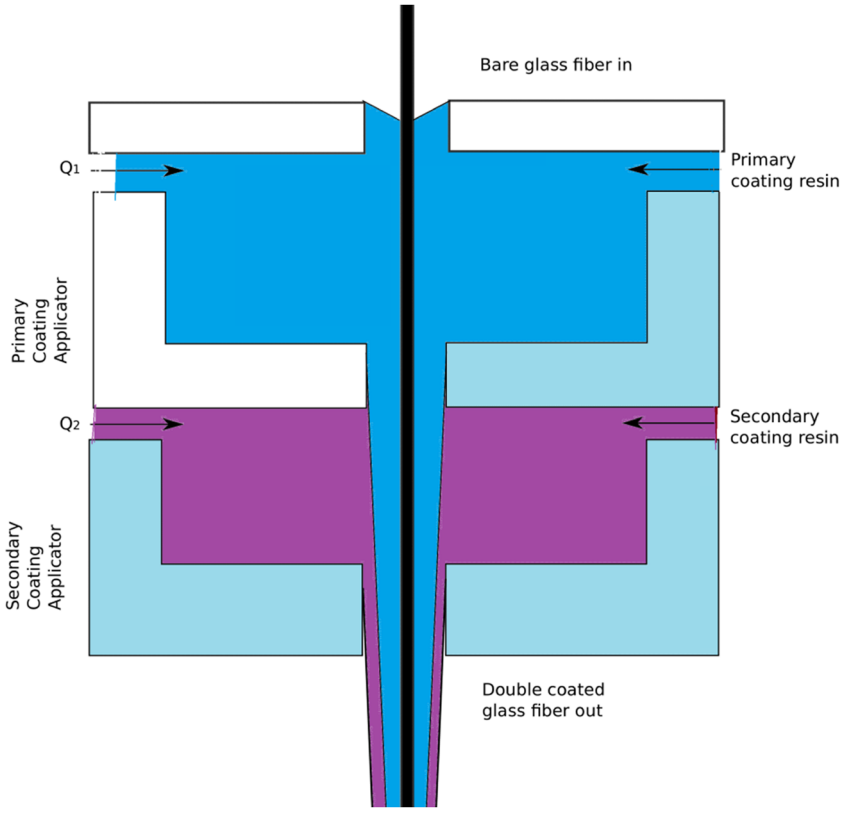

Figure 2: Two-phase flow model.

Momentum equation

$$\rho^{(\varphi)}\frac{\mathrm{D}\upsilon^{(\varphi)}}{\mathrm{D}t} = -\nabla\pi^{(\varphi)} + \Phi^{(\varphi)} + \vartheta^{(\varphi)} \times B^{(\varphi)}. \tag{2}$$

Energy equation

$$\chi_{\pi}^{(\varphi)}\frac{\mathrm{D}\Theta^{(\varphi)}}{\mathrm{D}t} = \kappa^{(\varphi)}\nabla^2\Theta^{(\varphi)} + \phi^{(\varphi)}, \tag{3}$$

where $\frac{\mathrm{D}}{\mathrm{D}t} = \frac{\partial}{\partial t} + \upsilon^{(\varphi)}$. ∇ is the substantive acceleration and $\upsilon^{(\varphi)}$ is the fluid velocity, $\rho^{(\varphi)}$ is the density, $\frac{\mathrm{D}}{\mathrm{D}\,t}$ is the material derivative, $\vartheta^{(\varphi)}$ represents the current density, $B^{(\varphi)}$ is the magnetic field strength, $\chi_{\pi}^{(\varphi)}$ is the specific heat, $\kappa^{(\varphi)}$ is the thermal conductivity parameter, and $\phi^{(\varphi)}$ is the dissipation function.

At the optical fiber and the die wall, no-slip boundary conditions are measured for velocity and temperature. The movement, shear force, differential pressure, heat, and heat transfer are all assumed to be uniform at the liquid interface.

The term $\vartheta^{(\varphi)} \times B^{(\varphi)}$ given in equation (2) is occurred because of the interaction of the magnetic pole. The electromagnetic force is caused by the fact that the charge density is low. The stunting effect per unit of volume traveling along the fiber optics is provided by a homogeneous magnetization in the upward radially perpendicular direction towards the fiber optics in z-direction as given below.

$$\vartheta^{(\varphi)} \times B^{(\varphi)} = (0,\ 0,\ -\sigma^{(\varphi)}B_0^2\upsilon^{(\varphi)}). \tag{4}$$

The Ohm's law in general form is updated to provide the Hall current whenever the magnetism is sufficiently strong. The value of current $J^{(j)}$ is provided, if the Hall element is preserved.

$$\vartheta^{(\varphi)} = \varepsilon^{(\varphi)}[\varsigma \times B_0 - \beta^{(\varphi)}(\vartheta^{(\varphi)} \times B_0)], \tag{5}$$

where $\varepsilon^{(\varphi)}$ is the fluid's electric conductivity and $\beta^{(\varphi)}$ is the Hall parameter. Equation (5) can be handled for magnetic Lorentz's effect $\vartheta^{(\varphi)}$ in the manner:

$$\vartheta^{(\varphi)} \times B_0 = -\frac{\varepsilon^{(\varphi)}B_0^2}{\mu^{(\varphi)2} + 1}\varsigma\kappa^{(\varphi)}, \tag{6}$$

where $\mu^{(\varphi)} = \varepsilon^{(\varphi)}\beta^{(\varphi)}B_0$ is the Hall factor, B_0 is the magnetic strength, and k is the unit vector along the z-direction.

The pertinent boundary and interface conditions for velocity field [14–19] are as given below:

$$\upsilon^{(1)} = V \ \text{ at } \ r = R_u, \ \ \upsilon^{(2)} = 0 \ \text{ at } \ r = R_d, \tag{7}$$

$$\upsilon^{(1)} = \upsilon^{(2)} \ \text{ and } \ S_{rz}^{(1)} = S_{rz}^{(2)} \ \text{ at } \ r = R. \tag{8}$$

The pertinent boundary and interface conditions for temperature field [16–19,57,58] are as follows:

$$\Theta^{(1)} = \Theta^{\exists(1)} \ \text{ at } \ r = R_w, \quad \Theta^{\exists(2)} = \Theta^{\exists(2)} \ \text{ at } \ r = R_d, \tag{9}$$

$$\Theta^{(1)} = \Theta^{(2)}, \quad K^{(1)}\frac{\mathrm{d}\Theta^{(1)}}{\mathrm{d}r} = K^{(2)}\frac{\mathrm{d}\Theta^{(2)}}{\mathrm{d}r} \ \text{ at } \ r = R. \tag{10}$$

Defining new variables

$$r^{\star} = \frac{r}{R_u}, \quad u^{*(j)} = \frac{\upsilon^{(\varphi)}}{V}, \quad \theta^{*(j)} = \frac{\Theta^{(\varphi)} - \Theta^{\exists(2)}}{\Theta^{\exists(2)} - \Theta^{\exists(1)}},$$

$$\tau_0^{(\varphi)} = \tau_2^{(\varphi)} + \tau_3^{(\varphi)}, \quad \frac{R_d}{R_u} = \delta > 1, \quad \frac{R}{R_u} = \Omega, \quad \lambda = \frac{\mu^{(2)}}{\mu^{(1)}},$$

$$K = \frac{\kappa^{(2)}}{\kappa^{(1)}},$$

Equations (2) and (3) in dimensionless form along with equations (7)–(10) become

$$r\frac{\mathrm{d}^2u^{(j)}}{\mathrm{d}r^2} + \frac{\mathrm{d}u^{(j)}}{\mathrm{d}r} + 2\beta^{(j)}\left(3r\frac{\mathrm{d}^2u^{(j)}}{\mathrm{d}r^2}\left(\frac{\mathrm{d}u^{(j)}}{\mathrm{d}r}\right)^2 + \left(\frac{\mathrm{d}u^{(j)}}{\mathrm{d}r}\right)^3\right) - \left(\frac{M^{2(j)}}{m^{2(j)} + 1}\right)u^{(j)}r = 0, \tag{11}$$

$$\frac{\mathrm{d}^2\theta^{(j)}}{\mathrm{d}r^2} + \frac{1}{r}\frac{\mathrm{d}\theta^{(j)}}{\mathrm{d}r} + \mathrm{Br}^{(j)}\left(\frac{\mathrm{d}u^{(j)}}{\mathrm{d}r}\right)^2 + 2\mathrm{Br}^{(j)}\beta^{(j)}\left(\frac{\mathrm{d}u^{(j)}}{\mathrm{d}r}\right)^4 = 0, \tag{12}$$

$$u^1(1) = 1, \quad u^2(\delta) = 0, \tag{13}$$

$$u^1 = u^2, \quad S_{rz}^1 = S_{rz}^1 \ \text{ at } \ r = \Omega, \tag{14}$$

$$\theta^1(1) = 0, \quad \theta^2(\delta) = 1, \tag{15}$$

$$\theta^1 = \theta^2, \quad \frac{\mathrm{d}\theta^1}{\mathrm{d}r} = \frac{K}{\delta}\frac{\mathrm{d}\theta^2}{\mathrm{d}r} \ \text{at } r = \Omega, \tag{16}$$

where $M^{2(j)} = \frac{\sigma^{(\varphi)}B_0^2R_u}{\mu^{(\varphi)}}$, $Br^{(j)} = \frac{\mu^{(\varphi)}V^2}{\kappa^{(\varphi)}(\Theta^{\exists(2)} - \Theta^{\exists(1)})}$, $\beta^{(j)} = \frac{\tau_0^{(\varphi)}}{\mu^{(\varphi)}\left(\frac{R_u^2}{V^2}\right)}$ are Magnetic parameter, Brinkman number, and non-Newtonian parameter, respectively [10–13,16–18].

3 Numerical solution procedure

To obtain numerical solutions for the set of boundary value systems defined in mathematical formulas (11)–(16), the fluid flow and temperature were analyzed for double coating of fiber optic employing non-Newtonian viscoelastic liquid, considering the impact of Hall current, Brinkman number, magnetic parameter, and non-Newtonian parameter

of third-grade fluid. The relevant modifications can be used for such objective.

$$u^{(1)} = y_1,\ u^{(1)'} = y_2,\ u^{(1)''} = y_2',\ u^{(2)} = y_3,\ u^{(2)'} = y_4,\ u^{(2)''} = y_4'$$
$$\theta^{(1)} = y_5,\ \theta^{(1)'} = y_6,\ \theta^{(1)''} = y_6',\ \theta^{(2)} = y_7,\ \theta^{(2)'} = y_8,\ \theta^{(2)''} = y_8'. \tag{17}$$

The nonlinear differential equations (11) and (12) are reduced to the set of first-order differential equations corresponding to the boundary and interface conditions (13)–(16) by employing expression (17). These are solved numerically using the RK4 technique and the shooting algorithm after transformation.

$$\frac{d^2u^{(j)}}{dr^2} = \frac{\left[\left(\frac{M^{2(j)}}{m^{2(j)}+1} + K\right)u^{(j)}r - \frac{du^{(j)}}{dr} - 2\beta^{(j)}\left(\frac{du^{(j)}}{dr}\right)^3\right]}{\left[r + 6\beta^{(j)}r\left(\frac{du^{(j)}}{dr}\right)^2\right]}, \tag{18}$$

$$\frac{d^2\theta^{(j)}}{dr^2} = -\left[\frac{1}{r}\frac{d\theta^{(j)}}{dr} + \mathrm{Br}^{(j)}\left(\frac{du^{(j)}}{dr}\right)^2 + 2\mathrm{Br}^{(j)}\beta^{(j)}\left(\frac{du^{(j)}}{dr}\right)^4\right], \tag{19}$$

$$y_2' = \frac{\left[\left(\frac{M^{2(1)}}{m^{2(1)}+1} + K\right)y_1 r - y_2 - 2\beta^{(1)}(y_2)^3\right]}{[r + 6\beta^{(1)}r(y_2)^2]},$$
$$y_4' = \frac{\left[\left(\frac{M^{2(2)}}{m^{2(2)}+1} + K\right)y_3 r - y_5 - 2\beta^{(2)}(y_4)^3\right]}{[r + 6\beta^{(2)}r(y_4)^2]}, \tag{20}$$

$$y_6' = -\left[\frac{1}{r}y_6 + Br^{(1)}y_6^2 + 2Br^{(1)}\beta^{(1)}y_6^4\right],$$
$$y_8' = -\left[\frac{1}{r}y_8 + Br^{(1)}y_8^2 + 2Br^{(2)}\beta^{(2)}y_8^4\right], \tag{21}$$

$$y_1(1) = 1,\ y_3(\delta) = 0,\ y_2(\Omega) = y_4(\Omega),\ y_1(\Omega) = y_3(\Omega),$$
$$y_5(1) = 0,\ y_7(\delta) = 1,\ y_5(\Omega) = y_7(\Omega),\ y_6(\Omega) = y_8(\Omega). \tag{22}$$

4 Result's confirmation

To validate the numerical results, the next assessments are performed, which demonstrate the suggested method's accuracy. Presented data and recently published article [21] were found to be in reasonable agreement. Figures 3 and 4 show a pictorial contrast of RK4 and HAM, respectively, for greater precision. Furthermore, Tables 1 and 2 demonstrate the comparison of the presented numerical solution, HAM solution, and published work [21] for fluid flow and heat transfer.

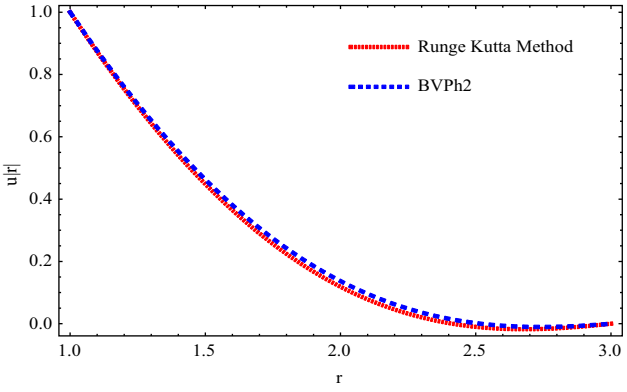

Figure 3: For velocity profiles, the RK-4 and BVPh2 approaches are compared.

5 Discussion

A brief research related to the emerging parameters that appear in this investigation has been schematically depicted and explained in Figures 5–13.

The influence of the magnetic field factor M on the velocity field is depicted in Figure 5. For higher amounts of the magnetic field parameter, a distinct reduction in velocity profile is investigated in the whole flow region. This is because when an electric field is applied to an electrical conductor liquid, the opposite force known as the Lorentz force increases.

The fluid velocity in the free surface segment is likely to be slowed by this frictional force. As the amount of the permeability parameter increases, the flow rate declines significantly, as shown in Figure 6. Figures 7 and 8 show how the fluid velocity is affected by the non-Newtonian parameter β and the Hall current factor m. Velocity

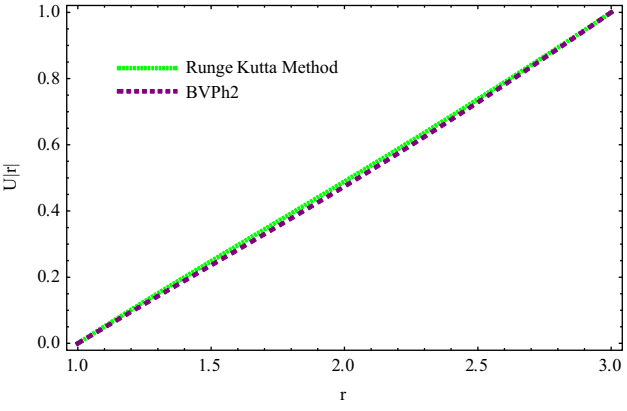

Figure 4: For temperature profiles, the RK-4 and BVPh2 approaches are compared.

Table 1: Velocity validation of the RK-4, BVPh2, and recently published work

$u(r)$	Numerical	HAM	[21]
1.0	1.00000	1.00000	1.00000
1.4	0.58216	0.58215	0.58212
1.8	0.537120	0.537121	0.537123
2.2	0.201835	0.201833	0.201832
2.6	0.010412	0.010410	0.010411
3.0	0.0000000	0.0000000	0.0000000

Table 2: Temperature validation of the RK-4, BVPh2, and recently published work

$\theta(r)$	Numerical	HAM	[21]
1.0	0.000000	0.000000	0.000000
1.4	0.35219	0.35218	0.35219
1.8	0.572106	0.572101	0.572106
2.2	0.861932	0.861930	0.861931
2.6	0.995621	0.995624	0.995621
3.0	1.0000000	1.0000000	1.0000000

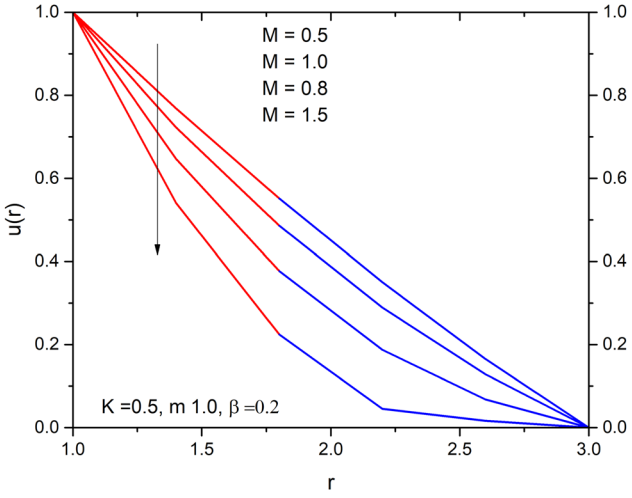

Figure 5: Influence of M on velocity profile.

profiles increase for both non-Newtonian and Hall current increasing parameters in the presence and absence of magnetic field M. We examine the effect of the magnetic field parameter on the temperature gradient $\theta(r)$ in Figure 9. It is observed that when the external magnetic field increases, the temperature distribution in the whole flow zone of the flowing fluid rises. This could be due to the bounding surface effects that outweigh the magnetic field impact.

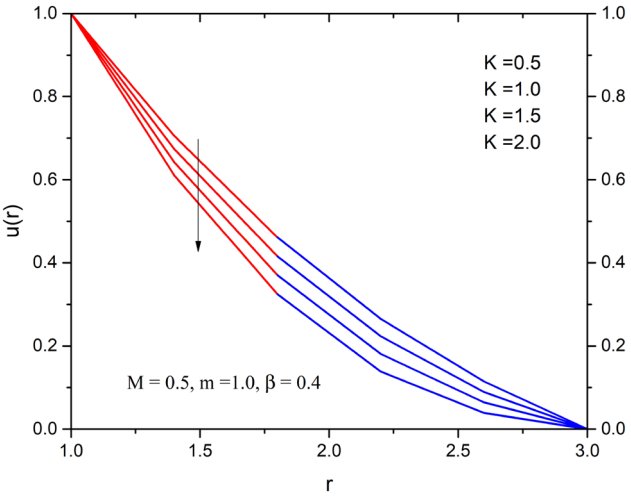

Figure 6: ; Influence of K on velocity profile.

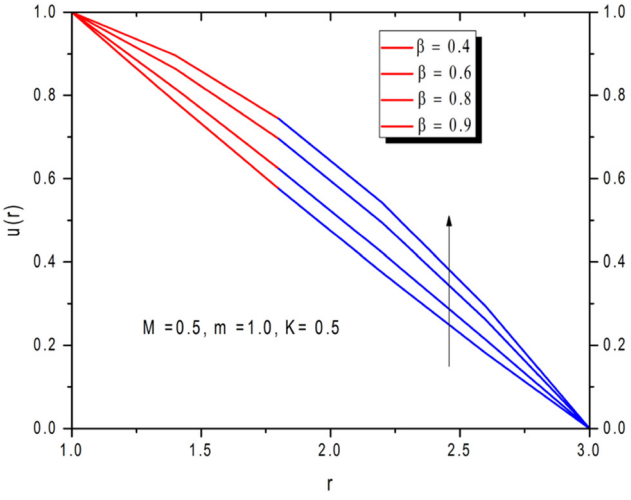

Figure 7: Influence of β on velocity profile.

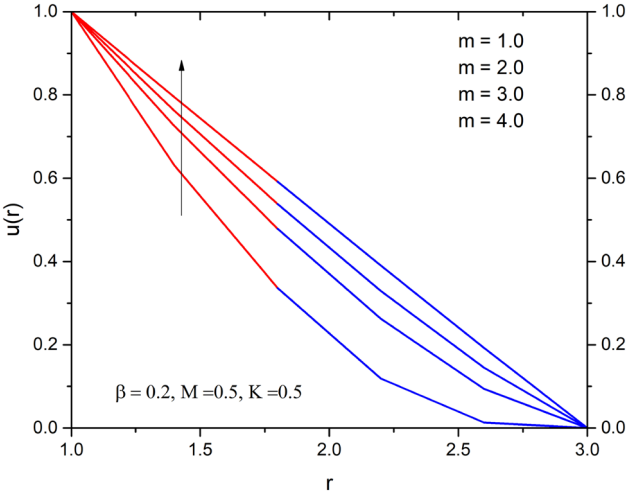

Figure 8: Influence of m on velocity profile.

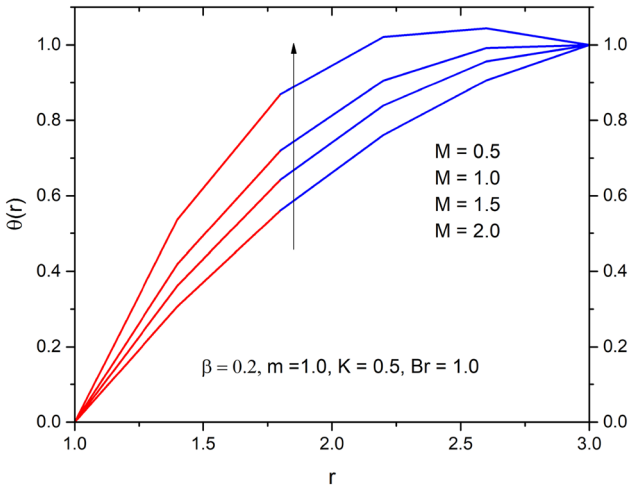

Figure 9: Influence of *M* on temperature profile.

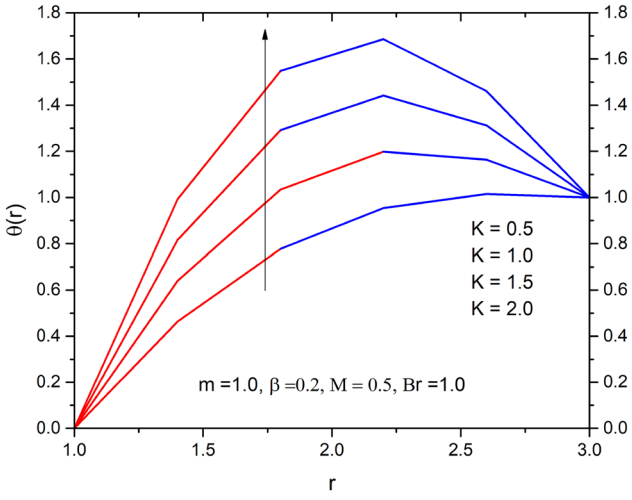

Figure 10: Influence of *K* on temperature profile.

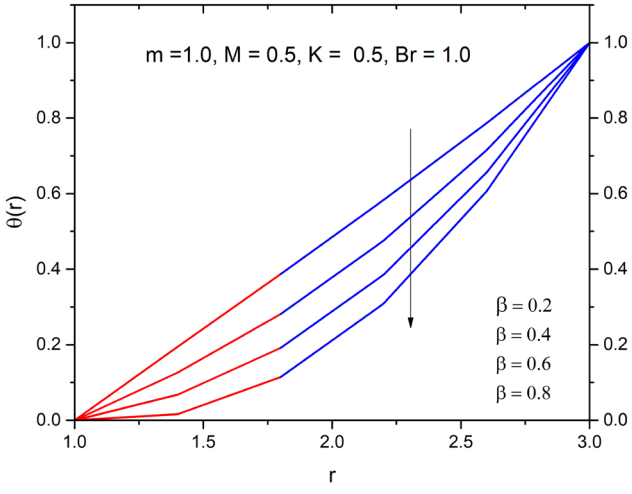

Figure 11: Influence of β on temperature profile.

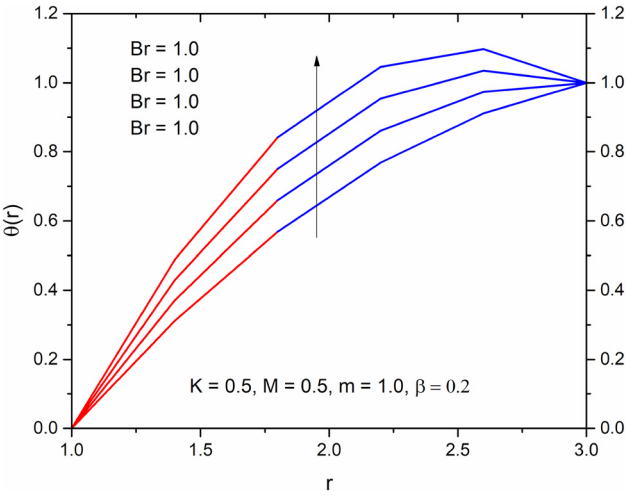

Figure 12: Influence of *Br* on temperature profile.

Figure 10 depicts the effect of the permeability factor on the temperature field. It is analyzed that greater amount of the permeability factor uniformly raises the fluid temperature inside the flowing zone. The effect of a non-Newtonian factor on temperature is depicted in Figure 11. It is noted that with greater amount of the non-Newtonian characteristic, a distinct decrease in heat transfer is noticed. Both in the existence and absence of magnetism, the non-Newtonian variable lowers the temperature profile. Figure 12 shows that when the Brinkman number *Br* rises, the temperature profile rises as well. The heat flux is found to grow dramatically at all places when the Brinkman number increases. As a result, it is noticed that throughout the wire surface coating, the temperature rapidly increases uniformly at all sites, as measured by the Brinkman number, which is the ratio of viscous heating to

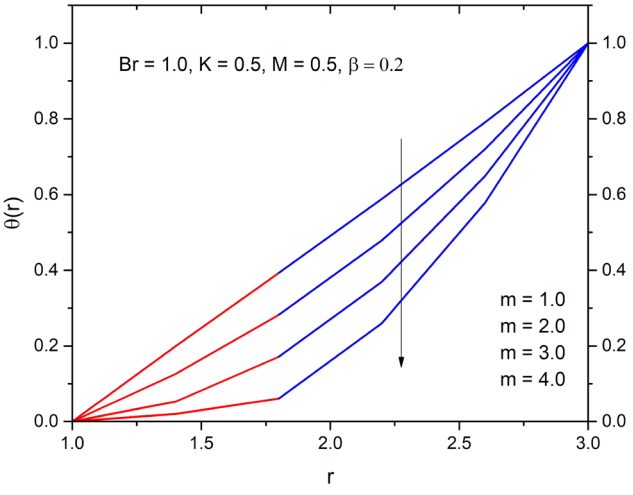

Figure 13: Influence of *m* on temperature profile.

the conductive heating. In the situation of a permeability parameter, the Hall factor lowers the temperature distribution, as shown in Figure 13.

6 Conclusion

In this investigation, we examined multiple coating assessments of fiber optics utilizing micro- polar convection third-order liquid including Hall current impact. In this research, the RK4-Fehlberg algorithm is applied to get numerical results for a list of nonlinear ODE describing liquid motion. Pictorially, the contribution of regulating variables on velocity and temperature profiles is examined. The suggested approach is compared to BVPh2 for verification purpose, and quivered is obtained. In addition, as a restricted scenario, a connection is made with the existing literature. The velocity field enhances with the rising value of β. It is observed that velocity profile increases as m enhances. For higher amounts of the magnetic field parameter, a distinct reduction in velocity profile is investigated in the whole flow region. This is because when an electric field is applied to an electrical conductor liquid, the opposite force known as the Lorentz force increases. It is observed that when the external magnetic field increases, the temperature distribution in the whole flow zone of the flowing fluid rises. This could be due to the bounding surface effects that outweigh the magnetic field impact. Both in the existence and absence of a magnetism, the non-Newtonian variable lowers the temperature profile. Furthermore, it is analyzed that when the Brinkman number Br rises, the temperature profile rises as well. The heat flux is found to grow dramatically at all places when the Brinkman number enhances, while opposite trend is observed for K and Br.

This work can be extended using the thin-film flow of various non-Newtonian viscoelastic fluids. Also, the Bingham Plastic fluid, Oldroyd 8-constant fluid are the viscoelastic non-Newtonian fluid can also be used for wire and double-layer coating of optical fiber. Similarly, the nanofluids and hybrid nanofluids can also be utilized in the base fluid for coating purpose in order to protect the wire and optical fiber from mechanical damage.

Funding information: The authors state no funding involved.

Author contributions: Z.K. modeled and solved the problem by RK4. I.K. validated the problem. A., N.A., and N.H. helped in revision, removed grammatical mistakes, and revised the whole manuscript. All authors have accepted responsibility for the entire content of this manuscript and approved its submission.

Conflict of interest: The authors state no conflict of interest.

References

[1] Nadeem S, Ahmad S, Muhammad N. Cattaneo–Christov flux in the flow of a viscoelastic fluid in the presence of Newtonian heating. J Mol Liq. 2017;237:180–4.
[2] Tabassum R, Mehmood R, Nadeem S. Impact of viscosity variation and micro rotation on oblique transport of Cu–water fluid. J Colloid Interface Sci. 2017;501:304–10.
[3] Nadeem S, Sadaf H. Exploration of single wall carbon nanotubes for the peristaltic motion in a curved channel with variable viscosity. J Braz Soc Mech Sci Eng. 2017;39:117–25.
[4] Shahzadi I, Sadaf H, Nadeem S, Saleem A. Bio-mathematical analysis for the peristaltic flow of single wall carbon nanotubes under the impact of variable viscosity and wall properties. Comput Methods Prog Biomed. 2017;139:137–47.
[5] Ijaz S, Shahzadi I, Nadeem S, Saleem A. A clot model examination: with impulsion of nanoparticles under influence of variable viscosity and slip effects. Commun Theor Phys. 2017;68(5):667.
[6] Poom K, Zahir S, Abdullah D, Haroon Ur R, Saeed I. Entropy generation in MHD radiative flow of CNTs Casson nanofluid in rotating channels with heat source/sink. Math Probl Eng. 2019;2019:9158093. doi: 10.1155/2019/9158093.
[7] Siddiqui AM, Mahmood R, Ghori QK. Thin film flow of a third grade fluid on a moving belt by He's homtopy perturbation method. Int J Non-Linear Sci Numer Simul. 2006;7:7–14.
[8] Siddiqui AM, Mahmood R, Ghori QK. Thin film flow of a third grade fluid on an inclined plane. Chaos Solitons Fractals. 2008;35:140–7.
[9] Akai M, Inoue A, Aokis S. The prediction of stratified two-phase flow with two-equation model of turbulence. Int J Multiph Flow. 1981;7:21–9.
[10] Shah RA, Islam S, Siddiqui AM, Haroon T. Heat transfer by laminar flow of an elastico-viscous fluid in post treatment analysis of wire coating with linearly varying temperature along the coated wire. J Heat Mass Transf. 2012;48:903–14.
[11] Shah RA, Islam S, Siddiqui AM, Haroon T. Optimal homotopy asymptotic method solution of unsteady second grade fluid in wire coating analysis. J Ksiam. 2011;15(3):201–22.
[12] Shah RA, Islam S, Siddiqui AM, Haroon T. Exact solution of differential equation arising in the wire coating analysis of an unsteady second grade fluid. Math Comp Mod. 2013;57:1284–8.
[13] Shah RA, Islam S, Ellahi M, Haroon T, Siddiqui AM. Analytical solutions for heat transfer flows of a third grade fluid in case of post-treatment of wire coating. Int J Phys Sci. 2011;6:4213–23.
[14] Kim K, Kwak HS, Park SH. Theoretical prediction on double-layer coating in wet-on-wet optical fiber coating process. J Coat Technol Res. 2011;8:35–44.

[15] Kim KJ, Kwak HS. Analytic study of non-Newtonian double layer coating liquid flows in optical fiber manufacturing. Trans Tech Publ. 2012;224:260–3.
[16] Zeeshan K, Islam Shah S, Siddique AM. Double-layer optical fiber coating using viscoelastic phan-thien tanner fluid. N Y Sci J. 2013;6:66–73.
[17] Zeeshan K, Shah RA, Khan I, Gul T. Exact solution of PTT fluid in optical fiber coating analysis using two-layer coating flow. J Appl Env Biol Sci. 2015;5:96–105.
[18] Zeeshan K, Islam S, Shah RA, Khan I, Gul T, Gaskel P. Double-layer optical fiber coating analysis by withdrawal from a bath of Oldroyd 8-constant fluid. J Appl Env Biol Sci. 2015;5:36–51.
[19] Khan Z, Islam S, Shah RA, Khan I. Flow and heat transfer of two immiscible fluids in double layer optical fiber coating. J Coat Technol Res. 2016;13(6):1055–63. doi: 10.1007/s1 1998-016-9817-1.
[20] Ellahi R, Rahman SU, Gulzar MM, Nadeem S, Vafai K. A mathematical study of non-Newtonian micropolar fluid in arterial blood flow through composite stenosis. Appl Math Inf Sci. 2014;8:1567–73.
[21] Hayat T, Nadeem S. Aspects of developed heat and mass flux models on 3D flow of Eyring–Powell fluid. Results Phys. 2017;7:3910–7.
[22] Hayat T, Nadeem S. Flow of 3D Eyring–Powell fluid by utilizing Cattaneo–Christov heat flux model and chemical processes over an exponentially stretching surface. Results Phys. 2018;8:397–403.
[23] Ijaz S, Nadeem S. A balloon model examination with impulsion of Cu-nanoparticles as drug agent through stenosed tapered elastic artery. J Appl Fluid Mech. 2017;10(6):1773–83.
[24] Ijaz S, Nadeem S. A biomedical solicitation examination of nanoparticles as drug agents to minimize the hemodynamics of a stenotic channel. Eur Phys J Plus. 2017;132(11):448.
[25] Saleem S, Nadeem S, Sandeep N. A mathematical analysis of time dependent flow on a rotating cone in a rheological fluid. Propuls Power Res. 2017;6(3):233–41.
[26] Mahanthesh B, Gireesha BJ, Gorla RSR. Unsteady three dimensional MHD flow of a nano Eyring–Powell fluid past a convectively heated stretching sheet in the presence of thermal radiation, viscous dissipation and Joule heating. J Assoc Arab Univ Basic Appl Sci. 2017;23:75–84.
[27] Rehman FU, Nadeem S. Heat transfer analysis for three-dimensional stagnation-point flow of water-based nanofluid over an exponentially stretching surface. J Heat Transf. 2018;140(5):7.
[28] Zeeshan K, Muhammad AK, Nasir S, Murad U, Qayyum S. Solution of magnetohydrodynamic flow and heat transfer of radiative viscoelastic fluid with temperature dependent viscosity in wire coating analysis. PLoS One. 2018;13(3):e0194196. doi: 10.1371/journal.pone.0194196.
[29] Khan N, Sultan F. Homogeneous–heterogeneous reactions in an Eyring–Powell fluid over a stretching sheet in a porous medium. Spec Top Rev Porous Media. 2016;7(1):15–25.
[30] Hayata T, Aslam N, Rafq M, Alsaadi FE. Hall and Joule heating effects on peristaltic flow of Powell–Eyring liquid in an inclined symmetric channel. Results Phys. 2017;7:518–28.
[31] Haroon Ur R, Zeeshan K, Saeed I, Ilyas K, Juan LGG, Waris K. Investigation of two-dimensional viscoelastic fluid with non-uniform heat generation over permeable stretching sheet with slip condition. Complexity. 2019;2019:3121896. doi: 10.1155/2019/3121896.
[32] Zeeshan K, Haroon Ur R, Tawfeeq AA, Muradullah, Ilyas K, Iskander T. Effect of magnetic field and heat source on upper-convected-maxwell fluid in a porous channel. Open Phys. 2018;2018(16):917–28.
[33] Nadeem S, Ahmad S, Muhammad N, Mustafa MT. Chemically reactive species in the flow of a Maxwell fluid. Results Phys. 2017;7:2607–13.
[34] Khan Z, Rasheed HU, Ullah M, Gul T, Jan A. Analytical and numerical solutions of Oldroyd 8-constant fluid in double-layer optical fiber coating. J Coat Technol Res. 2018;16(1):235–48. doi: 10.1007/s11998-018-0113-0.
[35] Rehman AU, Mehmood R, Nadeem S. Entropy analysis of radioactive rotating nanofluid with thermal slip. Appl Therm Eng. 2017;1122:832–40.
[36] Muhammad N, Nadeem S. Ferrite nanoparticles Ni-ZnFe2O4, Mn-ZnFe2O4 and Fe2O4 in the flow of ferromagnetic nanofluid. Eur Phys J Plus. 2017;132(9):312–21.
[37] Ijaza S, Nadeem S. Consequences of blood mediated nano transportation as drug agent to attenuate the atherosclerotic lesions with permeability impacts. J Mol Liq. 2018;262:565–75.
[38] Zeeshan K, Nasser T, Wali KM, Haroon Ur R, Habib S, Waris K. MHD and slip effect on two-immiscible third grade fluid on thin film flow over a vertical moving belt. Open Phys. 2019;2019(17):1–12.
[39] Rashid M, Shahzadi I, Nadeem S. Corrugated walls analysis in micro channels through porous medium under electromagnetohydrodynamic (EMHD) effects. Results Phys. 2018;9:171–82.
[40] Zeeshan K, Haroon Ur R, Iskander T, Ilyas K, Tariq A. Runge-Kutta 4th-order method analysis for viscoelastic Oldroyd 8-constant fuid used as coating material for wire with temperature dependent viscosity. Sci Rep. 2018;8(1):1–3. doi: 10.1038/s41598-018-32068-z.
[41] Zeeshan K, Waqar AK, Haroon Ur R, Ilyas K, Kottakkaran SN. Melting flow in wire coating of a third-grade fluid over a die using Reynolds' and Vogel's models with non-linear thermal radiation and joule heating. Materials. 2019;12(19):3074. doi: 10.3390/ma12193074.
[42] Zeeshan K, Haroon UR, Alharbi SO, Ilyas K, Tariq A, Dennis LCC. Manufacturing of double layer optical fiber coating using phan-thien tanner fluid as coating material. Coatings. 2019;9(2):147. doi: 10.3390/coatings9020147.
[43] Zeeshan K, Muhammad AK, Saeed I, Bilal J, Fawad H, Haroon Ur R, et al. Analysis of magneto-hydrodynamics flow and heat transfer of a viscoelastic fluid through porous medium in wire coating analysis. Mathematics. 2017;5:27. doi: 10.3390/math5020027.
[44] Zeeshan K, Rehan AS, Saeed I, Hamid J, Bilal J, Haroon Ur R, et al. MHD flow and heat transfer analysis in the wire coating process using elastic-viscous. Coatings. 2017;7:15. doi: 10.3390/coatings7010015.
[45] Khan Z, Rasheed HU, Ullah M, Khan I, Alkanhal TA, Tlili I. Shooting method analysis in wire coating withdrawing from a bath of Oldroyd 8-constant fluid with temperature dependent viscosity. Open Phys. 2018;16:956–66.
[46] Ijaz MK, Faris A, Aatef H, Zulfiqar A. Fully developed second order velocity slip Darcy-Forchheimer flow by a variable thicked surface of disk with entropy generation. Int Commun

Heat Mass Transf. 2020;117:104778. doi: 10.1016/j.icheatmasstransfer.2020.104778.
[47] Gireesha BJ, Sowmya G, Ijaz MK, Öztop HF. Flow of hybrid nanofluid across a permeable longitudinal moving fin along with thermal radiation and natural convection. Comput Methods Prog Biomed. 2020;185:105166. doi: 10.1016/j.cmpb.2019.105166.
[48] Khan M, Alsaedy A, Hayat T, Niaz BK. Modeling and computational analysis of hybrid class nanomaterials subject to entropy generation. Comput Methods Prog Biomed. 2019;179:104973. doi: 10.1016/j.cmpb.2019.07.001.
[49] Ramana Murthy V, Srinivas J, Sai KS. Flow of immiscible micropolar fluids between two porous beds. J Porous Media. 2014;7:287–300.
[50] Ramana Murthy JV. Anwar Bég 0. Entropy generation analysis of radiative heat transfer effects on channel flow of two immiscible couple stress fluids. J Braz Soc Mech Sci Eng. 2017:39:2191–202.